A Multispectral Fluorescence Imaging System: Design and Initial Clinical Tests in Intra-Operative Photofrin-Photodynamic Therapy of Brain Tumors

Victor X.D. Yang, MASc,[1] Paul J. Muller, MD,[2] Peter Herman, PhD,[3] and Brian C. Wilson, PhD[1,4]*
[1]*Department of Medical Biophysics, University of Toronto, Toronto, Canada*
[2]*Division of Neurosurgery, St. Michael's Hospital, Toronto, Canada*
[3]*Department of Electrical and Computer Engineering, University of Toronto, Canada*
[4]*Ontario Cancer Institute/University Health Network, Toronto, Canada*

Background and Objectives: Intra-operative identification of tumor by fluorescence may improve surgical resection or photodynamic therapy (PDT). A novel instrument was designed, constructed, and tested for this purpose.
Study Design/Materials and Methods: The instrument was designed to provide high-resolution, multi-spectral (five band) fluorescence imaging, and non-contact point spectroscopy, with long working distance (~50 cm), large field-of-view (~3 cm diameter), large depth of view (~2 cm), and 'point-and-shoot' operation. Its performance was determined in tissue-simulating phantoms and in pilot studies in brain tumor resection patients, with or without intra-operative Photofrin-PDT.
Results: In phantoms the imaging resolution was ~150 μm, while Photofrin concentrations as low as 0.05 or 0.1 μg/g could be detected at the tissue surface or at 0.5 mm depth, respectively. Red Photofrin fluorescence could be clearly visualized post radical resection in all PDT patients, with biopsy confirmation of residual tumor tissue in regions that were not seen as tumor under white light. Photobleaching of Photofrin during PDT was also demonstrated.
Conclusions: The system performed to specification under realistic operating conditions and could reveal unresected residual tumor tissue. It may be used for either PDT dosimetry/monitoring and/or for surgical guidance. Lasers Surg. Med. 32:224–232, 2003. © 2003 Wiley-Liss, Inc.

Key words: fluorescence; photodynamic therapy; surgical guidance; imaging; spectroscopy; brain tumors

INTRODUCTION

In vivo fluorescence can provide new tools for clinical oncology: screening and diagnosis of early-stage malignancy, defining tumor extent, and optimizing localized treatment of solid tumors [1]. Recent technological advances in light sources, high-sensitivity imaging detectors, and high-performance spectrographs, together with advances in digital imaging/processing, are enabling a wide variety of medical applications, including intra-operative surgical guidance.

Due to the aggressive growth pattern and the infiltrative nature of glioblastoma multiforme (GBM), clinical disease-free survival rarely exceeds 18 months, despite aggressive treatment by surgery, radiotherapy, and chemotherapy [2–6]. An important prognostic factor is the extent of resection [7–10]. A recent study in 416 GBM patients indicated that resection of 89% of the gross tumor is needed to impact survival, and that a significant advantage is associated with >98% resection [11]. Image-guided resection may contribute by enabling more precise and complete resection. For this purpose, CT and MRI offer superb pre-operative structural images, but intra-operative imaging is currently limited by shifts in the brain tissue due to retraction, resection, and cerebrospinal fluid drainage [12–15]. Intra-operative real-time imaging reduces these artifacts, but requires highly specialized systems coupled with robotic tools. Intra-operative ultrasound has been attempted [12,16], but is cumbersome for open-field use.

Optical imaging offers high-resolution, non-contact imaging. Fluorescence, in particular, also has the advantage of high sensitivity that allows rapid imaging with large field-of-view and potentially high tumor-to-normal tissue specificity. As reviewed by Wagnieres et al. [1], the development of in vivo fluorescence imaging has either used tissue autofluorescence or exogenous fluorophores (often photodynamic therapy (PDT) sensitizers). The optimum choice involves many factors and is often disease site- and stage-dependent. In general, autofluorescence usually is better for early-stage disease (dysplasia and carcinoma in situ), while the differential uptake/retention of photosensitizers has been more useful for late-stage bulk tumor delineation. The pro-drug aminolevulinic acid (ALA), which increases endogenous synthesis of the fluorescent

Contract grant sponsor: NIH P01 Program; Contract grant number: CA43892; Contract grant sponsor: Photonics Research Ontario; Contract grant sponsor: The Ontario Cancer Institute.
*Correspondence to: Dr. Brian C. Wilson, Rm 7-417, Ontario Cancer Institute, 610 University Ave., Toronto, Ont., M5G 2M9. E-mail: wilson@uhnres.utoronto.ca
Accepted 8 September 2002
Published online in Wiley InterScience (www.interscience.wiley.com).
DOI 10.1002/lsm.10131

photosensitizer protoporphyrin IX (PpIX), appears to have potential for detecting both early and late-stage disease.

There have been a few studies of fluorescence in brain tumors. Murray et al. [17] provided one of the early clinical reports of fluorescence in surgical resection, while Poon et al. [18] reported intraoperative use of exogenous (phthalocyanine) fluorescence pre-clinically, with positive results. Kabuto et al. [19] used fluorescein and a modified operating microscope in both animal and clinical studies, and autofluorescence was attempted by Bottiroli et al. intraoperatively [20]. Recently, Stummer et al. [21] reported the development and evaluation of a fluorescence imaging system incorporated into a surgical microscope, using ALA–PpIX (375–440 nm excitation, >455 nm detection). Tests in a series of patients [22] showed that fluorescence-guided resection was technically feasible and that the completeness of resection, determined by residual tissue fluorescence, was related to the post-operative MRI findings.

We have pursued a different technological approach, by developing a free-standing fluorescence camera independent of the operating microscope, and this paper reports its design and initial clinical tests. The main rationale was to develop a general surgical tool, rather than one that is integrated into a specific neurosurgical microscope. This allows greater flexibility in optical design and functionality, so that the system can be optimized for imaging the fluorescence rather than the white-light reflectance. The potential disadvantages are discussed below.

We previously reported [23] preclinical studies with an earlier prototype of the system. For this, the detection matrix of a charge coupled device (CCD) camera was split into three regions: two square areas for imaging and a rectangular strip for spectroscopy. This allowed simultaneous dual-wavelength imaging and full spectroscopy, but the image resolution was limited by the resulting small matrix size. Hence, here we have used the complete detector area for imaging, with sequential selection in different wavelength bands, and with part of the light split off into a separate spectrograph and point detector. After describing the construction and performance of this multispectral fluorescence imaging (MFI) system, we will present a preliminary clinical demonstration in detecting residual tumor following surgical resection of GBM, performed as part of Phase III clinical trials of PDT using Photofrin™ (QLT, Vancouver, BC, Canada) [24].

MATERIALS AND METHODS

System Design and Performance Measurements

The MFI system is an optical illumination and imaging instrument specifically designed for use during open-field surgical procedures. It is capable of both fluorescence imaging in multiple emission wavelength bands and point fluorescence emission spectroscopy. The key functional features are:

1) capability to switch between white light imaging and fluorescence imaging in multiple emission wavelength bands;
2) co-axial fluorescence illumination and detection, so that the system functions as a 'point and shoot' fluorescence camera, with the light emitted from the head such that the illuminated area is always coincident with the imaging field-of-view;
3) long working distance, large field-of-view, and depth of focus;
4) point fluorescence spectroscopy with user-controlled selection of the measurement position within the image field;
5) high sensitivity and resolution.

Figure 1 shows the imaging and spectroscopy optical paths of the instrument, while Figure 2 shows the camera head mounted on a suspension arm in the operating room. A 150 W mercury lamp (EFOS, Mississauga, Ont., Canada) provides an irradiance of 2.8 mW/cm^2 at the image plane. A pass-band filter selects the fluorescence excitation band: for Photofrin this is set at 405 ± 15 nm (Omega, Brattleboro, NJ) to match the absorption spectrum (Fig. 3). The filtered beam is focused to a uniform beam at ~50 cm in front of the objective lens (D = 120 mm, f = 235 mm, Melles Griot, Irvine, CA) of the camera head, illuminating the resection cavity uniformly (the excitation intensity variation is <15% within the field of view). The fluorescence is collected by the same lens and separated by a 50:50 beam splitter into either the imaging or spectroscopy optical paths. For imaging, the light passes through one of five filters mounted on a filter wheel (Oriel, Stratford, CT). For Photofrin the filters used were centered at 495, 543, 600, 640, and 720 nm (Omega), each with approximately 20 nm bandwidth. This combination of filters allowed measurement of blue, green, and red light for both white-light and fluorescence imaging, as well as detecting the background autofluorescence around the 640 nm Photofrin emission peak. After passing through folding optics to minimize the size of the camera head, the light is focused onto a 6.4 × 4.8 mm CCD detector (DVC, Austin, TX). This operates at

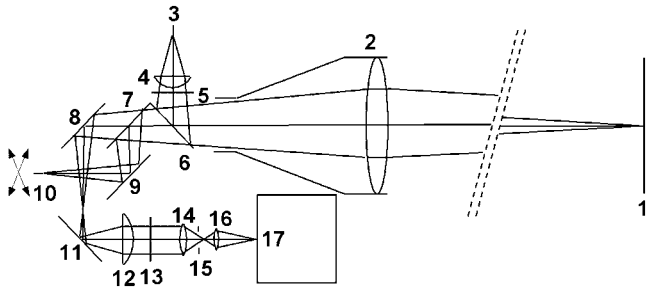

Fig. 1. Optical layout of the imaging head. 1, object plane; 2, primary objective lens (f = 235 mm, D = 120 mm); 3, liquid light guide from the mercury lamp; 4, plano-convex lens (f = 38 mm, D = 25.4 mm); 5, excitation filter ($\lambda_{pass} = 405 \pm 15$ nm, D = 25.4 mm); 6, dichroic long-pass filter ($\lambda_{cut\,off} = 475$ nm, D = 50.8 mm); 7, 50:50 beam splitter; 8,9,11, planar mirrors (D = 50.8 mm); 10, motorized fiber-optic coupler to spectrograph; 12, plano-convex lens (f = 100 mm, D = 50.8 mm); 13, filter wheel; 14, 15, and 16, C-mount lens; 17, CCD.

Fig. 2. Photograph of the camera (with sterile drapes) in the operating theatre.

room temperature and has 755×484 pixels with 10-bit resolution. The field of view is 3.3×2.5 cm and the depth of focus is 2 cm. In operation, the five filters are automatically selected in turn with a switching time of $\sim$1 second and integration time of $\sim$2 seconds. The MFI system can also take white-light images of the surgical field, using normal operating room ambient lighting.

In the spectroscopy optical path, the light is dispersed by a grating spectrograph and detected by a photodiode array (Ocean Optics, Dunedin, FL). The detection spot in the image plane over which the spectrum is measured is 0.6 mm diameter. The position in the image field-of-view at which the fluorescence emission spectrum is collected is selected by a joystick controller. The spectral resolution is approximately 20 nm FWHM over the range of 500–700 nm. The output of the CCD and point spectroscopy are digitized in real-time to a personal computer, which displays the white-light and fluorescence images as well as the spectra.

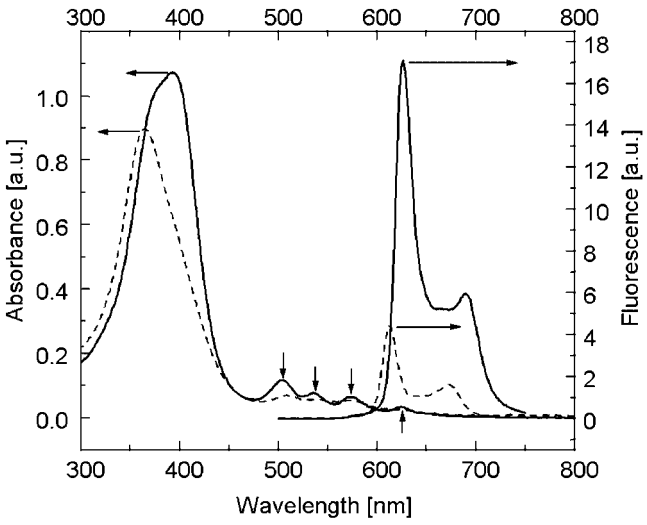

Fig. 3. Absorption and fluorescence (405 nm excitation) spectra of aggregated Photofrin (dash line) in distilled water and monomerized Photofrin in methanol (solid line). Small arrows indicate the Q-band absorption peaks.

The resolution, depth of view, and sensitivity of the imaging system was determined as follows. Collagen fluorescence transmitted through a standard US Air Force resolution target was used to measure the fluorescence modulation transfer function. Tissue-simulating phantoms were prepared from Trypan Blue and microspheres to approximate brain tissue optical properties. Different concentrations of Photofrin in a capillary tube submerged in the phantom were used to test the sensitivity of the imaging system.

Clinical Tests

These tests were carried out with IRB approval from St. Michael's Hospital and with informed patient consent. As part of existing phase-III randomized prospective clinical trials of PDT in the treatment of supratentorial gliomas using Photofrin [24], four patients (two male, two female, age 40–57) were imaged by the MFI system. Two additional patients (#1, 6) with benign cystic meningioma or recurrent cervical chordoma were also imaged (see Table 1). For patients undergoing PDT, 2 mg/kg of Photofrin was administered i.v. 24 hours before the surgery. The entire surgical cavity was then irradiated at 630 nm using a balloon irradiator to uniformly scatter the light, delivering either 40 or 120 J/cm^2 to the resection surface.

The positioning of the MFI system in the operating room was similar to that of a conventional operating microscope with manual suspension arms. The operating microscope was also used when necessary for the surgical resection. After resection, the MFI was focused onto the base of the resection cavity. Prior to taking images, the surgical field was irrigated to remove residual blood [23], which could significantly attenuate the fluorescence excitation light. A complete MFI measurement included a white-light image, a corresponding fluorescence image, and a fluorescence spectrum. The white-light image was taken with the operating room lights on. The fluorescence image and spectroscopy were obtained with the operating room lights turned off for a short period (<1 minute), and the imaging system's own excitation light on, controlled with a foot pedal. During a typical operation, two complete MFI measurements were made, one after the surgical resection and one after the PDT. Biopsies were taken from the tumor resection cavity and examined histologically and by fluorescence spectrofluorimety to determine the pathology and Photofrin concentration, respectively.

In the fluorescence images, the red tissue autofluorescence at 640 ± 20 nm was calculated by linearly interpolating the fluorescence spectra in the 600 ± 20 and 710 ± 20 nm bands. This background was then subtracted to produce a false-color composite image optimized for viewing the characteristic red Photofrin fluorescence centered at around 640 nm (Fig. 3). Due to the small

TABLE 1. Patient Data

Patient number	Diagnosis	Lacalization and lesion diameter	PDT
1	Benign cystic meningioma	Left frontal, 5 cm	No
2	Cystic astrocytoma mixed with GBM[a]	Left frontal and temporal, 5 cm	Yes
3	Recurrent GBM	Right frontal, 5 cm	Yes
4	GBM	Right parietal, 4 cm	Yes
5	GBM	Right occipital, 5 cm	Yes
6	Recurrent chordoma	C4–C5, 6 cm	No

[a]GBM, glioblastoma multiforme.

sample size in this pilot study (N = 6), statistical analysis was not attempted. Photobleaching was examined in one PDT patient (#3), in whom three complete MFI procedures were carried immediately before, during, and immediately after the PDT light administration.

The histological diagnosis was performed by a neuropathologist blinded to the treatment. The Photofrin concentration in the tissue was measured using an established technique [25], comprising solubilization of the sample followed by measurement of the fluorescence signal in a calibrated spectrofluorimeter (Photon Technology, Lawrenceville, NJ).

RESULTS

System Performance

The modulation transfer function is shown in Figure 4a. Over the entire field of view, the spatial resolution, defined at the 50% MTF, is approximately 0.15 mm, or six line pairs per mm. Using tissue phantoms with optical absorption and scattering properties similar to brain tissue in the red ($\mu_a = 2.2\ cm^{-1}$, $\mu'_s = 9.3\ cm^{-1}$), the minimum concentration (at 1:1 signal to noise ratio) of Photofrin detectable by the imaging system was 0.05 μg/g at the tissue surface and 0.1 μg/g at 0.5 mm below the surface, as shown in Figure 4b. These performance figures need to be confirmed in the clinical setting by systematic evaluation in a series of patients with, for example, MRI confirmation of the imaging resolution, and such studies are planned.

Clinical Tests

The fluorescence image acquisition time was typically ~15 seconds for all five wavelength bands in both white-light and fluorescence modes. Spectroscopy took ~1 second per point for a signal-to-noise ratio of 10 at the peak fluorescence emission. Histology of the biopsy samples confirmed four patients with GBM (World Health Organization Grade IV), one patient with benign cystic meningioma, and one patient with chordoma, as per Table 1.

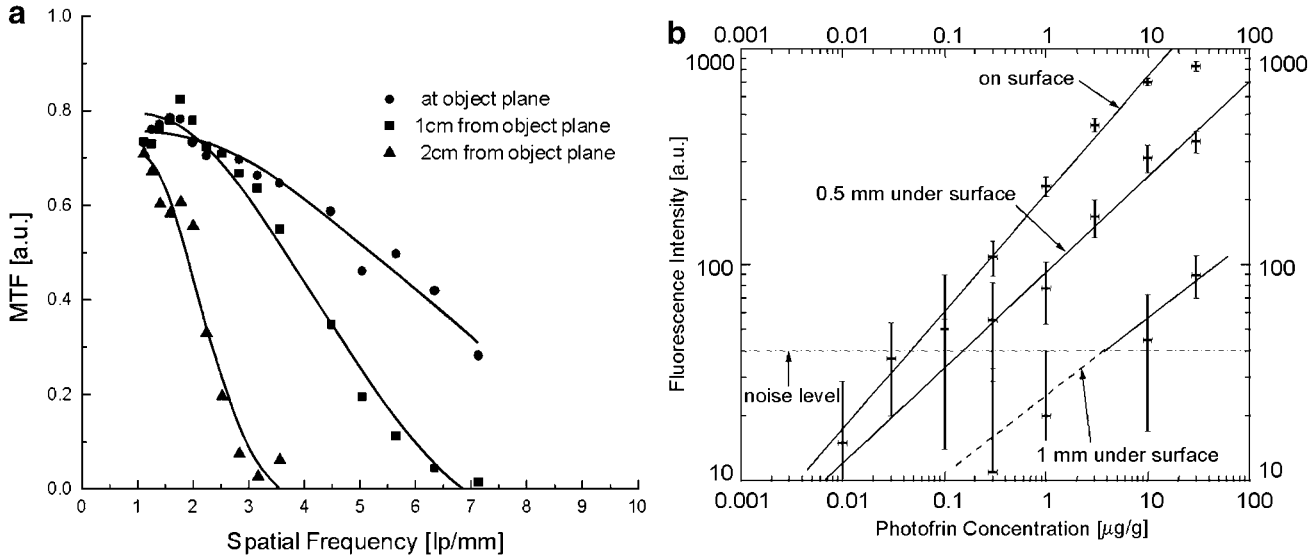

Fig. 4. Performance measurements. **a**: Fluorescence modulation transfer function measured with the resolution target placed at different distances from the focal plane in air. The solid curves are Gaussian fits to the experimental data points. Within the depth of focus (±1 cm), the MTF was >10% at 6.5 line pairs per mm (~0.15 mm spatial resolution). **b**: Detected fluorescence intensity versus Photofrin concentration in tissue-simulating phantoms ($\mu_a = 2.2\ cm^{-1}$, $\mu'_s = 9.3\ cm^{-1}$ at 630 nm) at the surface and at depth below the surface. The horizontal line corresponds to a unity signal-to-noise ratio.

Intraoperatively, GBM tissue in the resection cavity showed strong characteristic red fluorescence, as shown in the example in Figure 5. Small, well-defined papillary projections of the red fluorescence region were visible in the image, shown in Figure 5b, consistent with the infiltrative nature of this tumor. The biopsy sample taken from the region with bright red fluorescence were confirmed as malignant, while the Photofrin concentration measured ex vivo was 9.5 ± 0.4 μg/g. The surrounding tissue, which showed less red fluorescence and appeared green in the composite image was histologically normal and showed a porphyrin concentration of 0.8 ± 0.2 μg/g. There was no visible tumor present in the corresponding white-light image, shown in Figure 5a.

After complete surgical resection under white-light condition, regions with residual red fluorescence were observed in all four PDT patients. These regions ranged from sub-millimeter to about 10 mm in size. After PDT treatment, residual red fluorescent regions were found in two patients (#3, 5). These regions were biopsied and histological assessment showed vascular proliferation (#3) and GBM (#5). Assessment of photobleaching was carried out on one patient (#3) from images obtained before, during, and after PDT irradiation (Fig. 6). In this case, the red fluorescence decreased during the treatment, while the green fluorescence intensity increased. Since only three time points were measured during the treatment, we performed a single exponential fit to the red fluorescence and obtained a photobleaching rate constant of $\beta = 0.04 \pm 0.02$ cm^2/J, comparable to published values for Photofrin in other tissues, which range from 0.004 to 0.036 cm^2/J [26,27]. The increase in green fluorescence may have been due to reduced blood content in the tissue as a result of the vascular effects of PDT [28], leading to reduced attenuation of the short-wavelength fluorescence.

Connective tissue rich in collagen and elastin fibers, such as bone and dura, appeared green in the composite fluorescence image, as would be expected from the known fluorescence spectra of these molecules [1]. Also as expected with blue light excitation, blood markedly attenuated the green fluorescence, with surface blood vessels being visible and hyperemic regions (identified from the white-light images) appearing dark in the fluorescence images in patients not injected with Photofrin (as in the cases of

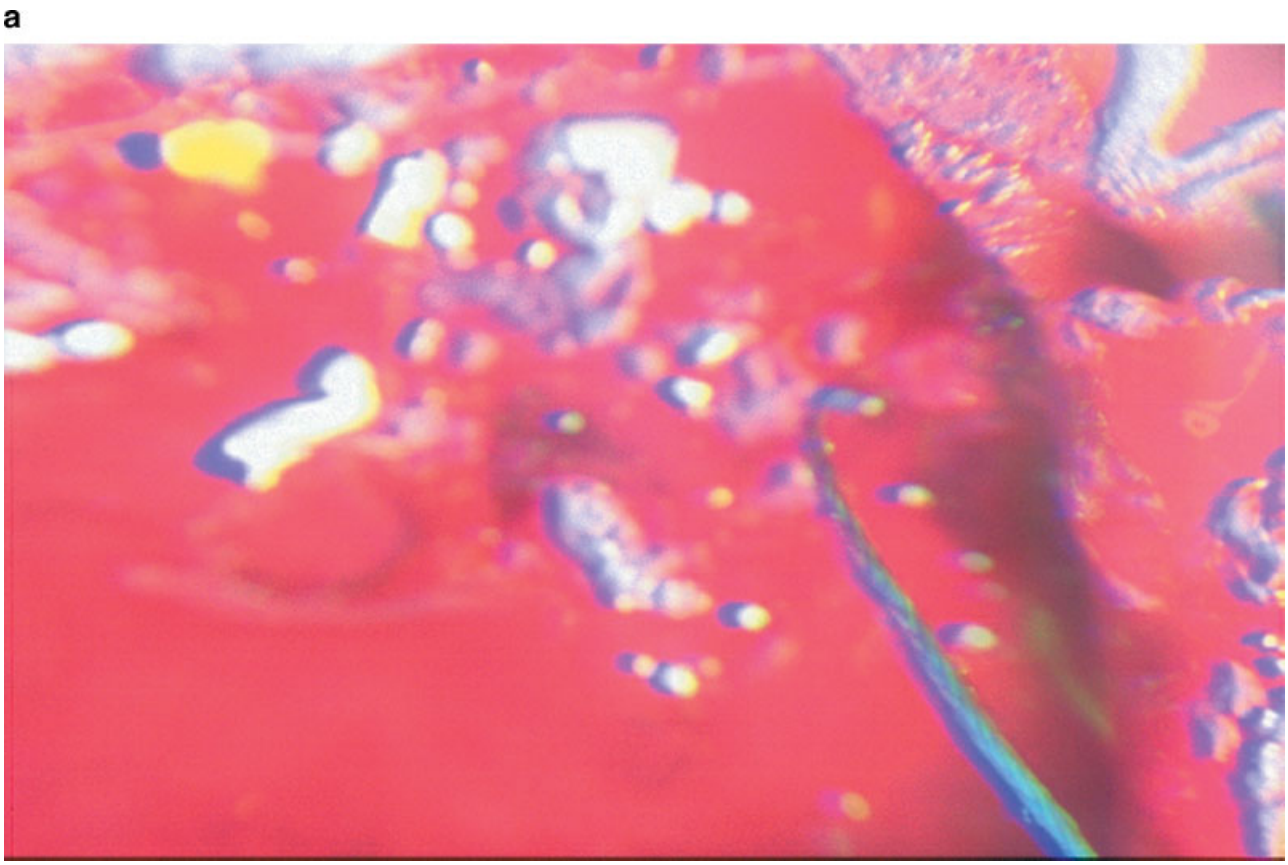

Fig. 5. Images in patient #4. **a**: White-light image (3.3 × 2.5 cm) of the resection cavity, with a cotton string as spatial marker. Residual blood in the resection cavity caused the overall red appearance. **b**: Corresponding fluorescence image showing GBM regions with bright red fluorescence. Note the small, well-defined red regions (arrows) projecting outward.

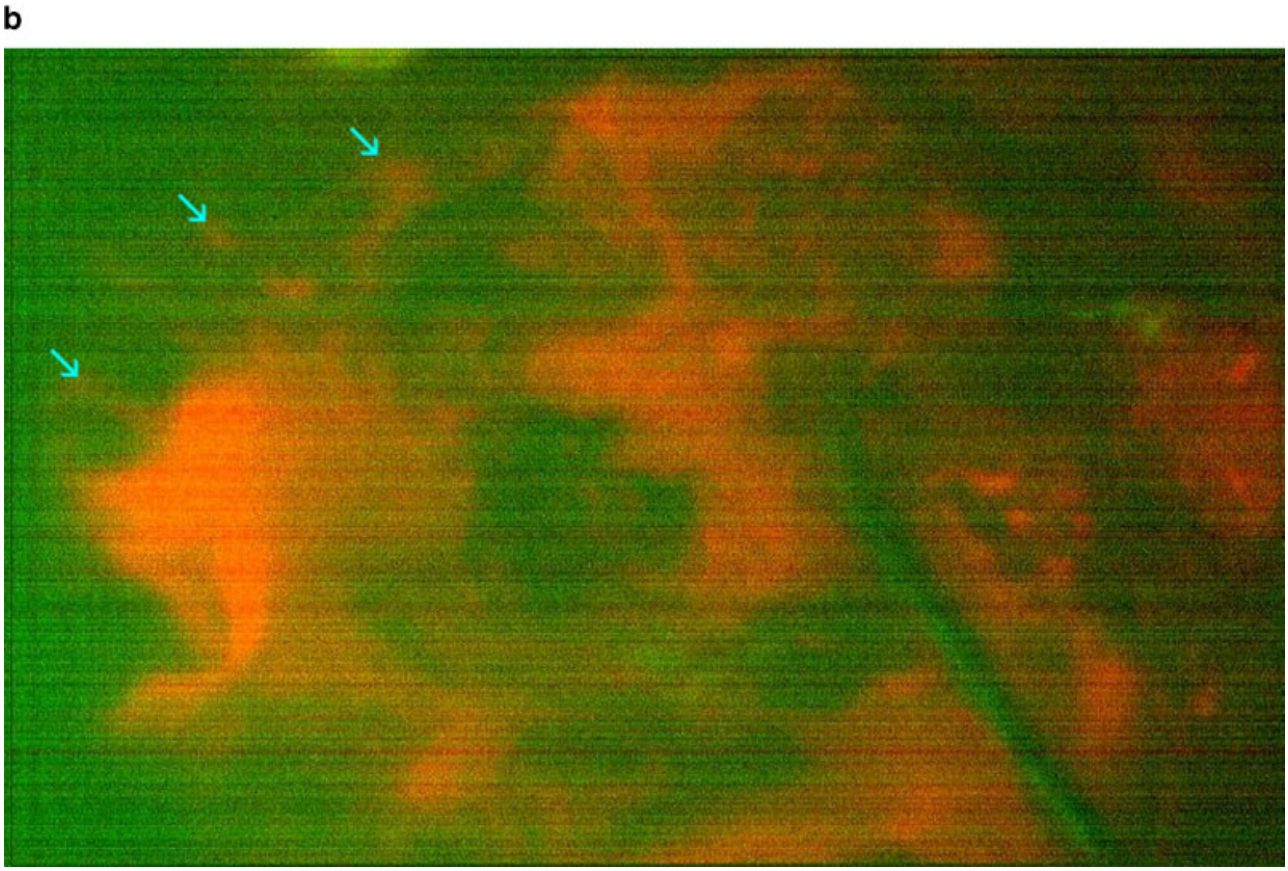

Fig. 5. (*Continued*)

meningioma and chordoma). Metallic surgical instruments appeared dark, while cotton swabs had bright green fluorescence, and served as convenient location markers during imaging.

DISCUSSION

The observations in this small group of patients suggest that the red Photofrin fluorescence may correlate with the presence of minimal (sub-millimeter) residual malignant tissue. Hence, the fluorescence could be used to guide surgical resection and promote better tumor tissue removal in silent areas of the brain, which could in turn improve survival rate, as suggested also by the data of Stummer et al. [21,22] using a surgical microscope modified for fluorescence imaging, in which the completeness of resection determined by fluorescence was related to postoperative MRI findings and to survival in GBM patients.

A particular advantage of the MFI system is that it is intrinsically capable of determining absolute fluorescence levels intraoperatively (with a signal-to-background ratio of about 10:1 in this study), since the target-to-detector geometry can be maintained between patients and the system gain is fixed. In particular, the target-to-detector distance is nearly constant if the tissue in focus, since the depth of field (~2 cm) is small compared to the working distance (50 cm). Because of the nearly flat-field illumination and the digital processing incorporating normalization of each fluorescence spectral window to the excitation, quantitative comparison between images can be made, even between patients. This applies also to the point fluorescence spectra measurements. The quantitative capability would, for example, allow an objective and reproducible threshold level of drug fluorescence to be set for the accurate identification of tumor. Determining this optimum threshold to give the maximum tumor tissue

Fig. 6. Images in patient #3. **A**,**D**: Before, (**B**,**E**) during, and (**C**,**F**) immediately after (120 J/cm^2) of PDT light irradiation. Image field of view = 3.3 × 2.5 cm. A–C: White light images. D–F: Corresponding fluorescence images showing Photofrin photobleaching. **G**: Fluorescence intensity measured in the circled area, demonstrating photobleaching of the red fluorescence and an increase in the green fluorescence.

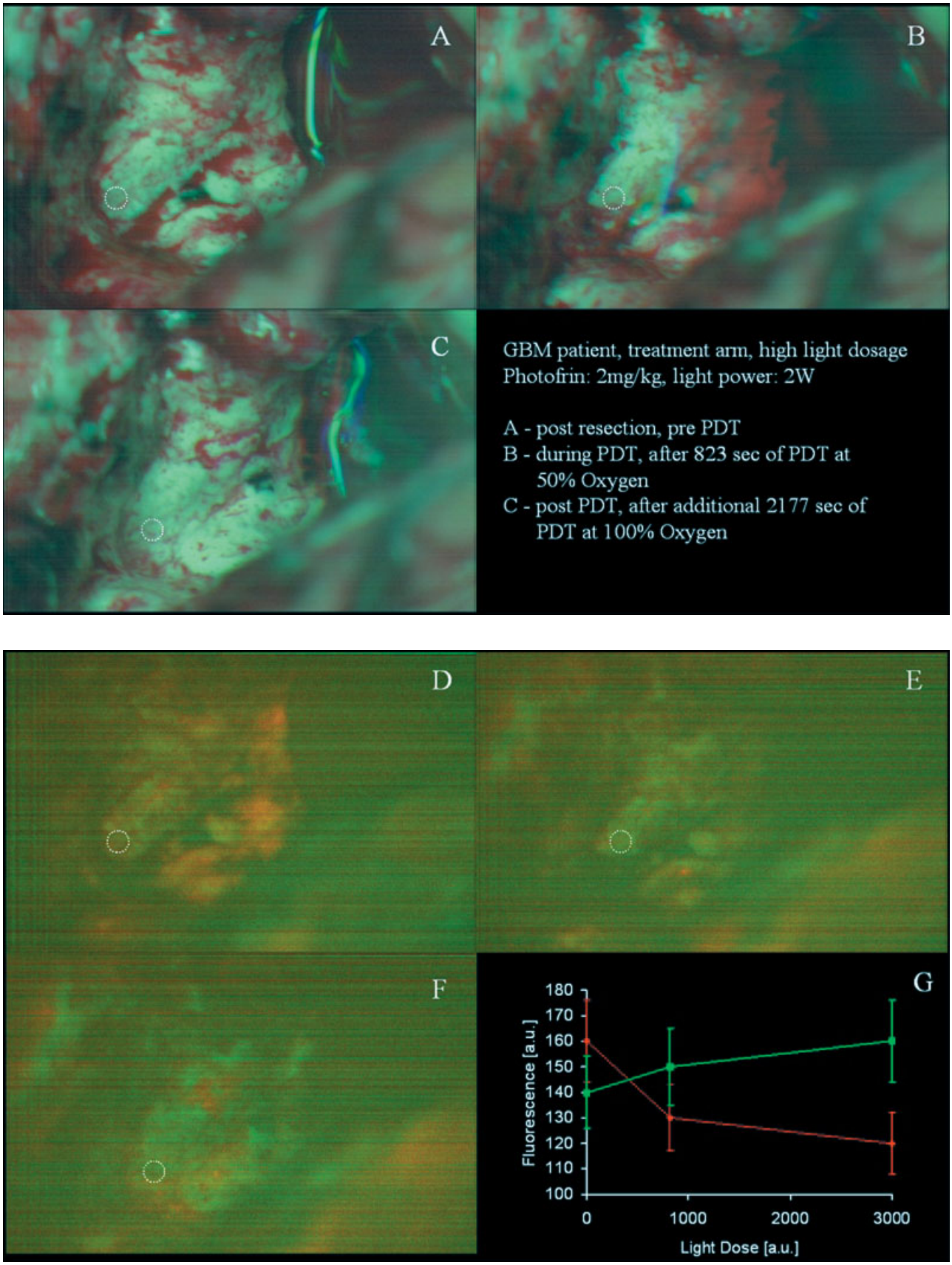
A
B
C
GBM patient, treatment arm, high light dosage
Photofrin: 2mg/kg, light power: 2W
A - post resection, pre PDT
B - during PDT, after 823 sec of PDT at 50% Oxygen
C - post PDT, after additional 2177 sec of PDT at 100% Oxygen
D
E
F
G
Fluorescence [a.u.]
180
170
160
150
140
130
120
110
100
0
1000
2000
3000
Light Dose [a.u.]

Fig. 6.

detection sensitivity and/or specificity will require clinical studies with each fluorophore.

The MFI has flexibility, in terms of selection of the fluorescence excitation and emission filters, to use a variety of fluorescent drugs. Such studies are in progress, both clinically and in animal models, for ALA-induced PpIX fluorescence, based on our previous observations of very high selectivity of ALA-mediated PpIX synthesis in tumor versus white matter [29]. In this case, the same filters can be used as for Photofrin.

Residual fluorescence in unresectable or "eloquent" areas detected by the MFI system may be an indication for the use of PDT post resection [24,25], and in addition to its potential utility in guiding the resection, the quantitative fluorescence imaging/point spectroscopy is also expected to be useful in optimizing PDT treatments. In on-going Phase-III Photofrin-PDT trials of malignant brain tumors [24], the administered Photofrin dose is fixed (2 mg/kg), and the light dosimetry is based on the resection cavity size, aiming to deliver a fixed incident fluence to the resection surface (40 or 120 J cm^{-2}) calculated from the laser output and the cavity diameter. However, the differential uptake of Photofrin between tumor and normal brain tissue is only $\sim$10:1, and preclinical studies suggest that normal brain tissue may be intrinsically more sensitive to Photofrin-PDT than the tumor tissue [24,29]. Hence, if one could determine the areas of residual tumor by fluorescence imaging, it is possible that targeting the light could maintain the tumor response while minimizing normal tissue damage. In principle, this light could be delivered through the MFI system itself, for example by a scanning laser beam or optical multi-leaf collimator analogous to radiotherapy [32]. The system could also be used to determine the pre-PDT photosensitizer concentration, allowing for adjustment of the light fluence to compensate for patient-to-patient (or even location-to-location) variations in this. Similarly, it has been proposed that intraoperative photobleaching measurement could be used for PDT dosimetry [27], integrating some of the response-determining factors into a single 'PDT dose metric' [30]. The MFI system provides a technical platform for this, as demonstrated in Figure 6.

In a more general sense, an optical intra-operative detection system such as the MFI could be combined with pre-operative or intra-operative CT or MRI imaging. The advantages are its very high resolution and sensitivity in detecting minimal residual disease. The fluorescence provides information only for the surface tissue layer ($<\sim$1 mm), although the depth sensitivity could be increased by using longer wavelength (near-IR) fluophores or by using sub-surface fiber-optic probes [33]. Hence, these features provide complementary information to radiological imaging methods, so that, for example, intra-operative CT or MRI could be used to guide the tumor debulking and fluorescence imaging/spectroscopy then used to guide the final resection of residual tumor tissue that cannot be seen radiologically or visually. The additional cost would also modest ($\sim$\$100 K) compared to CT or MRI.

We note finally that the design of the MFI as a freestanding unit allows it to be used in a wide range of surgical sites beyond neurosurgery, and we have carried out preliminary tests, for example, in the oral cavity. The multispectral capability allows easy adaptation to other fluorescent agents and its high sensitivity would enable tracer quantities of fluorophore to be used, such as might be available with fluorescence-labeled antibodies [34], and we have recently tested this in preliminary tumor-bearing animal studies. The main disadvantage of the freestanding approach is the frequent switching between the MFI system and the surgical microscope during the operations. Another disadvantage is the non-real time image acquisition due to the filter wheel movements, which can be avoided by using multiple imaging sensors as in the case of our ongoing work. For body sites where the working distance and/or field-of-view can be smaller, the optical design is easily scalable and we are building a compact prototype version of the system.

ACKNOWLEDGMENTS

These clinical studies were supported by NIH P01 Program Grant CA43892. The system development costs were supported by Photonics Research Ontario and the Ontario Cancer Institute. The Department of Biomedical Engineering, St. Michael's Hospital provided technical support. The authors also thank Dr. I. Taylor, Dr. P. Poldre of the Faculty of Medicine, Dr. A. Vitkin, Dr. L. Lilge of the Department of Medical Biophysics, University of Toronto for helpful discussions. Patents are pending.

REFERENCES

1. Wagnieres GA, Star WM, Wilson BC. In vivo fluorescence spectroscopy and imaging for oncological applications. Photochem Photobiol 1998;68:603–632.
2. Dirks P, Bernstein M, Muller PJ, Tucker WS. The value of reoperation for recurrent glioblastoma. Can J Surg 1993;36: 271–275.
3. Durmaz R, Erken S, Arslantas A, Atasoy MA, Bal C, Tel E. Management of glioblastoma multiforme with special reference to recurrence. Clin Neurol Neurosurg 1997;99:117–123.
4. Barker FG, Chang SM, Gutin PH, Malec MK, McDermott MW, Prados MD, Wilson CB. Survival and functional status after resection of recurrent glioblastoma multiforme. Neurosurgery 1998;42:709–723.
5. Halligan JB, Stelzer KJ, Rostomily RC, Spence AM, Griffin TW, Berger MS. Operation and permanent low activity 125I brachytheraphy for recurrent high-grade astrocytomas. Int J Radiat Oncol Biol Phys 1996;35:541–547.
6. Chandler KL, Prados MD, Malec M, Wilson CB. Long-term survival in patients with glioblastoma multiforme. Neurosurgery 1993;32:716–720; discussion 720.
7. Ammirati M, Vick N, Liao YL, Ciric I, Mikhael M. Effect of the extent of surgical resection on survival and quality of life in patients with supratentorial glioblastomas and anaplastic astrocytomas. Neurosurgery 1987;21:201–206.
8. Lai DM, Lin SM, Tu YK, Kao MC, Hung CC. Therapy for supratentorial malignant astrocytomas: Survival and possible prognostic factors. J Formos Med Assoc 1993;92:220–226.
9. Devaux BC, O'Fallon JR, Kelly PJ. Resection, biopsy, and survival in malignant glial neoplasms: A retrospective study of clinical parameters, therapy, and outcome. J Neurosurg 1993;78:767–775.

10. Kowalczuk A, Macdonald RL, Amidei C, Dohrmann G, Erickson RK, Hekmatpanah J, Krauss S, Krishnasamy S, Masters G, Mullan SF, Mundt AJ, Sweeney P, Vokes EE, Weir BK, Wollman RL. Quantitative imaging study of extent of surgical resection and prognosis of malignant astrocytomas. Neurosurgery 1997;41:1028–1036; discussion 1036–1038.
11. Lacroix M, Abi-Said D, Fourney DR, Gokaslan ZL, Shi W, DeMonte F, Lang FF, McCutcheon IE, Hassenbusch SJ, Holland E, Hess K, Michael C, Miller D, Sawaya R. A multivariate analysis of 416 patients with glioblastoma multiforme: Prognosis, extent of resection, and survival. J Neurosurg 2001;95:190–198.
12. Zakhary R, Keles GE, Berger MS. Intraoperative imaging techniques in the treatment of brain tumors. Curr Opin Oncol 1999;11:152–156.
13. Kelly PJ. Image-directed tumor resection. Neurosurg Clin N Am 1990;1:81–95.
14. Aronen HJ, Cohen MS, Belliveau JW, Fordham JA, Rosen BR. Ultrafast imaging of brain tumors. Top Magn Reson Imaging 1993;5:14–24.
15. Kraus GE, Bernstein TW, Satter M, Ezzeddine B, Hwang DR, Mantil J. A technique utilizing positron emission tomography and magnetic resonance/computed tomography image fusion to aid in surgical navigation and tumor volume determination. J Image Guid Surg 1995;1: 300–307.
16. Woydt M, Horowski A, Krone A, Soerensen N, Roosen K. Localization and characterization of intracerebral cavernous angiomas by intra-operative high-resolution colour duplex sono-graphy. Acta Neurochir (Wien) 1999;141:143–151; discussion 152.
17. Murray KJ. Improved surgical resection of human brain tumors: Part I. A preliminary study. Surg Neurol 1982;17: 316–319.
18. Poon WS, Schomacker KT, Deutsch TF, Martuza RL. Laser-induced fluorescence: Experimental intraoperative delineation of tumor resection margins. J Neurosurg 1992;76:679–686.
19. Kabuto M, Kubota T, Kobayashi H, Nakagawa T, Ishii H, Takeuchi H, Kitai R, Kodera T. Experimental and clinical study of detection of glioma at surgery using fluorescent imaging by a surgical microscope after fluorescein administration. Neurol Res 1997;19:9–16.
20. Bottiroli G, Croce AC, Locatelli D, Nano R, Giombelli E, Messina A, Benericetti E. Brain tissue autofluorescence: An aid for intraoperative delineation of tumor resection margins. Cancer Detect Prev 1998;22:330–339.
21. Stummer W, Stocker S, Wagner S, Stepp H, Fritsch C, Goetz C, Goetz AE, Kiefmann R, Reulen HJ. Intraoperative detection of malignant gliomas by 5-aminolevulinic acid-induced porphyrin fluorescence. Neurosurgery 1998;42: 518–525; discussion 525–526.
22. Stummer W, Novotny A, Stepp H, Goetz C, Bise K, Reulen HJ. Fluorescence-guided resection of glioblastoma multiforme by using 5-aminolevulinic acid-induced porphyrins: A prospective study in 52 consecutive patients. J Neurosurg 2000;93:1003–1013.
23. Yang VXD, Yeow J, Lilge L, Kost J, Mang T, Wilson BC. Non-contact point spectroscopy guided by two-channel fluorescence imaging in a hamster cheek pouch model. Proc Soc Photo-Opt Instr Eng 1999;3595:2–8.
24. Muller P, Wilson B, Lilge L, Yang VXD, Fullagar T, Hetzel F, Chen Q, Fenstermaker R, Selkar R, Abrams J. Clinical trials in photodynamic therapy of malignant brain tumors. Proc Soc Photo-Opt Instr Eng 2000;3909:15–24.
25. Lilge L, O'Carroll C, Wilson BC. A solubilization technique for photosensitizer quantification in ex vivo tissue samples. Photochem Photobiol 1997;B39:229–235.
26. Boyle DG, Potter WR. Photobleaching of Photofrin II as a means of eliminating skin photosensitivity. Photochem Photobiol 1987;46:997–1001.
27. Mang TS, Dougherty TJ, Potter WR, Boyle DG, Somer S, Moan J. Photobleaching of porphyrins used in photodynamic therapy and implications for therapy. Photochem Photobiol 1987;45:501–506.
28. Engbrecht BW, Menon C, Kachur AV, Hahn SM, Fraker DL. Photofrin-mediated photodynamic therapy induces vascular occlusion and apoptosis in a human sarcoma xenograft model. Cancer Res 1999;59:4334–4342.
29. Lilge L, Olivo MC, Schatz SW, MaGuire JA, Patterson MS, Wilson BC. The sensitivity of normal brain and intracranially implanted VX2 tumor to interstitial photodynamic therapy. Br J Cancer 1996;73:332–343.
30. Wilson BC, Weerskin RA, Lilge L. Fluorescence in photodynamic therapy dosemetry Ch. 20. In: Pogue B, Mycek M, editors. Fluorescence in biomedicine. NY: Marcel Dekker; 2003 in press.
31. Wilson BC, Patterson MS, Lilge L. Implicit and explicit dosimetry in photodynamic therapy: A new paradigm. Lasers Med Sci 1997;12:182–199.
32. Russell NS, Bartelink H. Radiotherapy: The last 25 years. Cancer Treat Rev 1999;25:365–376.
33. Daneshvar MI, Peralta JM, Casay GA, Narayanan N, Evans L, Patonay G, Strekouski L. Detection of biomolecules in the near-infrared spectral region via a fiber-optic immunosensor, J Immunol Methods 1999;226:119–128.
34. Kostler WJ, Brodowicz T, Hejna M, Wiltschke C, Zielinski CC. Detection of minimal residual disease in patients with cancer: A review of techniques, clinical implications, and emerging therapeutic consequences. Cancer Detect Prev 2000;24:376–403.